

Generating quantum feature maps using multi-objective genetic algorithm

Haiyan Wang*

School of Mathematical and Natural Science, Arizona State University, Phoenix, AZ 85069, USA

Allison Bayro†

*School of Biological and Health Systems Engineering,
Arizona State University, Tempe, AZ 85287, USA*

Nao Yamamoto‡

Department of Population Health, New York University Grossman School of Medicine, New York, NY 10016, USA

We present a novel approach for efficiently generating quantum feature maps for quantum-enhanced support vector machines, a kernel-based classifier, enabling access to high-dimensional Hilbert space. Our method employs a multi-objective genetic algorithm that simultaneously maximizes classification accuracy while minimizing both the local and non-local gate costs of the quantum feature map's circuit. To achieve this, we define distinct fitness functions for local gates and entanglement gates. Comparisons with classical classifiers are given in order to understand the advantages of using quantum machine learning. Surprisingly, our experiments reveal that the optimal configuration of quantum circuits for the quantum kernel method incorporates a proportional number of non-local gates for entanglement, contrary to previous literature where non-local gates were largely suppressed.

Furthermore, we demonstrate that the separability indexes of data can be effectively leveraged to determine the number of non-local gates required for the quantum support vector machine's feature maps. This insight can significantly aid in selecting appropriate parameters, such as the entanglement parameter, in various quantum programming packages like quiskit.org based on data analysis. Our findings offer valuable guidance for enhancing the efficiency and accuracy of quantum machine learning algorithms.

Keywords: support vector machine; quantum feature map; genetic algorithm; entanglement gate

1. INTRODUCTION

Quantum machine learning (QML) stands out as one of the most promising and fascinating applications of quantum technologies. Both machine learning and quantum computing have the potential to revolutionize computation and tackle previously intractable problems. In the realm of pattern recognition, kernel methods, especially support vector machines (SVMs), have become widely recognized for their effectiveness in classification tasks. In recent years, kernel estimation SVM has emerged as a leading technique in this field. In this pursuit of quantum advantage, the quantum kernel method via support vector machine has emerged as a powerful approach, drawing attention from various research groups [4, 5, 7, 13, 14, 16, 21, 22, 24, 25, 27, 29, 31, 32, 46]. This method leverages high-dimensional quantum state spaces, allowing for enhanced computational capabilities.

In [14], two innovative strategies were proposed for designing quantum SVMs: the Quantum Kernel Estimator and the Quantum Variational Classifier. These strategies leverage classical data and encode it into the quantum state space using a quantum feature map. A key component of this process is the quantum circuit, which transforms the dataset from its original low-dimensional real space to a higher-dimensional quantum state space, also known as the Hilbert space [30].

Designing an efficient quantum circuit is crucial to explore the Hilbert space effectively and encode probability distributions efficiently while minimizing gate cost and circuit size to mitigate quantum noise. The choice of a suitable feature map, corresponding to an appropriate kernel, plays a pivotal role in the success of the kernel method. Depending on the dataset to be classified, the selection of an appropriate feature map becomes critical. Recent advancements [3, 8–11] have introduced the automatic generation of quantum feature maps through the utilization of multi-objective genetic algorithms. These algorithms offer a powerful approach to optimize the gate or circuit structure and avoid common pitfalls like local minima and barren plateaus [34–36]. By employing genetic algorithms to search for optimal quantum feature maps, researchers can significantly enhance the performance of quantum SVMs, driving them closer to practical applicability and expanding the scope of quantum machine learning.

* Corresponding author: haiyan.wang@asu.edu

† abayro@asu.edu

‡ Nao.Yamamoto@nyulangone.org

In previous works [3, 11], the design of feature maps has predominantly led to a suppression of entanglement gates. However, entanglement, a fundamental concept in quantum mechanics, plays a pivotal role in enabling quantum computing and understanding its mathematical formulation is crucial. To address this limitation, we propose a novel approach using three-objective genetic algorithms. Unlike the methods in [3, 11], we separate the optimization functions for local gates and non-local (controlled-NOT (CNOT)) gates. By doing so, we obtain a set of non-dominated points that reveal a more balanced configuration of quantum circuits for the quantum kernel method, incorporating a proportional number of CNOT gates to facilitate entanglement. Further analysis of this three-dimensional set of non-dominated points offers deeper insights into the feature map design.

The results of this paper indicate that various separability indexes can be used to help assessing the construct efficient quantum circuits for achieving high accuracy. Currently, the documentations for quantum kernels at qiskit.org do not provide a guide for how these parameters should be chosen. For example, the entanglement parameter of ZZFeatureMap has three options: linear, full and circular. The results of this paper can be used to help choosing these parameters based on analysis of data.

Key new contributions of this paper are 1) designing a genetic algorithms with three-objective functions to demonstrate that the entanglement gates are needed to achieve high prediction accuracy, which improves/complements the result in [3, 11] that the entanglement gates are not needed. 2) experimentally demonstrate that the correlation between separability indexes of data and the number of entanglement gates, which provides a useful guide for the use of the relevant packages in qiskit.org [2].

The paper is organized as follows. Section 2 presents a short literature review on related topics in quantum machine learning. A brief review of support vector machine and quantum kernel method is presented in Section 3. Section 4 describes the genetic algorithm in more details, including how we encode the problem and how we optimize the multi-objective fitness function. Section 5 explains the encoding scheme of quantum feature maps as binary strings of genes and fitness functions. Section 6 presents the results of applying the algorithm to breast cancer and Iris datasets, and how the separability indexes affect non-local gates. Finally, we have some discussion on our conclusions in Section 7.

2. LITERATURE REVIEW

Quantum machine learning represents a burgeoning area of study that seamlessly integrates advancements in quantum computing hardware and algorithms with concepts and challenges stemming from the realm of artificial intelligence. The field is experiencing both steady and rapid progress, showcasing a substantial repository of algorithms and applications already developed [4, 7, 14, 16, 22, 29, 31, 32, 46]. Quantum classifiers are a captivating technique, represented by the function $f(x) = \text{Tr}[\rho_x \rho_w]$, which encodes a data point \mathbf{x} in a quantum state using the feature map $|0\rangle\langle 0| \mapsto U(\mathbf{x})|0\rangle\langle 0| = \rho_x$, and encodes the weight vector through the mapping $|0\rangle\langle 0| \mapsto W|0\rangle\langle 0| = \rho_w$. This function serves as a linear model [38], making it ideal for supervised learning tasks. By using a parametric weight mapping $W(\theta)$, the parameters can be trained using gradient-descent-based techniques, leading to the concept of a quantum neural network [39, 40]. However, the training phase of these models may be affected by barren plateaus [41, 42], where the gradient variance diminishes exponentially with the number of qubits. Factors such as noise [43], global measurement [44], and expressibility of the feature map [45] have been associated with barren plateau occurrences. To address this issue, the Quantum Kernel Estimation (QKE) [14, 30, 37] algorithm can be hybridly employed by implementing a quantum kernel function $\kappa(\mathbf{x}, \mathbf{x}') = \text{Tr}[\rho_x \rho_{x'}]$, quantifying similarity between two encoded data points, and using it in conjunction with a classical machine learning algorithm. The model's training is classical and is expected to be successful and efficient due to the representer theorem [61]. Classical kernel methods have been fundamental in machine learning, applied to various tasks like signal processing [62–64], bioinformatics [64, 65], and image processing [66, 67].

Although the advantages of using quantum kernel estimation to enhance machine learning applications are still being explored [46], quantum kernels have shown performance improvements in classical machine learning problems, such as predicting the output of quantum systems [68, 69], and learning from distributions based on the discrete logarithm [70]. These quantum kernels have been successfully applied to real-world, industrial scale tasks, including anomaly detection [47], fraud detection [71–74], effectiveness of pharmaceutical treatments [75], and supernova classifications [76]. Experimental evaluations on superconducting [76] and optical [48] quantum devices are typically used to assess their effectiveness empirically.

Many of these experiments share a common structure: dimensionality reduction techniques to limit quantum resource requirements, input scaling, choice of quantum kernel, and evaluation. Researchers often develop software prototypes, requiring knowledge of diverse software frameworks and platforms, including those for machine learning tasks [49, 50] and quantum computing [51–55]. As prototypes grow, the risk of introducing bugs in the code increases [56], potentially leading to erroneous results [59, 60]. Well-organized code has been shown to facilitate code reuse and reproducibility [57, 58], providing benefits in research efficiency, reduced learning time, and deploying software for

production environments.

A key problem of parameterized circuit is their design, both from the point of view of the structure of the circuit as well as their parameterization. The structure and design condition the expressive power of the circuit [15], and its capacity to explore the Hilbert space and encode probability distributions more efficiently than other generative models. However, too expressive circuits can be subject to local minima and barren plateaus [41] that prevent reaching the optimal parameterizations. Partial solutions to these challenges include adaptive initialization strategies [3, 8–11] that optimize gates or structure.

3. SUPPORT VECTOR MACHINE WITH QUANTUM KERNELS

3.1. Support vector machine

Support vector machine (SVM) is a widely used classical supervised classification model in machine learning. Suppose we have a set of data points $\{(x_i, y_i) \mid x_i \in \mathbb{R}^n, y_i = \pm 1\}$, SVM finds a pair of parallel hyperplane $w \cdot x + b = \pm 1$ that divides the data points into two classes, where the decision boundary corresponds to the hyperplane $w \cdot x + b = 0$ with orientation controlled by w and offset controlled by b . The goal is to differ the data points by classes as much as possible, i.e., maximize the margin (distance) between the parallel hyperplane, where we can express the problem as $\min \frac{1}{2} \|w\|_2^2$ s.t. $y_i(w \cdot x_i + b) \geq 1$. The optimization problem for the primal problem can be formulated into Lagrange dual problem:

$$\begin{aligned} \max \quad & L(w, b, \alpha) = \sum_{i=1}^n \alpha_i - \frac{1}{2} \sum_{i=1}^n \sum_{j=1}^n \alpha_i \alpha_j y_i y_j x_i x_j \\ \text{s.t.} \quad & \sum_{i=1}^n \alpha_i y_i = 0, \quad \alpha_i \geq 0 \end{aligned} \tag{1}$$

The main goal of SVMs is to find decision boundaries to separate a given set of data points into classes. When these data spaces are not linearly separable, SVMs can benefit from the use of kernels to find these boundaries. Formally, decision boundaries are hyperplanes in a high dimensional space. When the data points are not linearly separable, we use a feature map ϕ to map the data into high dimensional space for more features or to low dimensional space to eliminate unimportant features. The kernel trick is to offer a more efficient and less expensive way to transform data into higher dimensions, where the data can be linearly separated in the higher dimensional space. The kernel function, denoted as $K(x_i, x_j) = \phi(x_i) \phi(x_j)$, allows us to perform SVM by just knowing how to calculate the inner product of $\phi(x_i)$ and $\phi(x_j)$ instead of knowing what the feature map ϕ is. In particular, the radial basis function (RBF) kernel, i.e., the Gaussian kernel is often used. Applying the kernel trick, we can rewrite the Lagrange dual problem:

$$\begin{aligned} \max \quad & L(w, b, \alpha) = \sum_{i=1}^n \alpha_i - \frac{1}{2} \sum_{i=1}^n \sum_{j=1}^n \alpha_i \alpha_j y_i y_j K(x_i, x_j) \\ \text{s.t.} \quad & \sum_{i=1}^n \alpha_i y_i = 0, \quad \alpha_i \geq 0 \end{aligned} \tag{2}$$

3.2. Quantum kernel method

Kernel methods are a collection of pattern analysis algorithms that use kernel functions to operate in a high-dimensional feature space. The best-known application of kernel methods is in SVMs, supervised learning algorithms commonly used for classification tasks. The kernel function implicitly maps input data into this higher dimensional space, where it can be easier to solve the initial problem. In other words, kernels may allow data distributions that were originally non-linearly separable to become a linearly separable problem. This is an effect known as the “kernel trick”. The Quantum Kernel Estimator in [14] proposed effective strategies to design a quantum SVM, namely and the Quantum Variational Classifier. [14] encodes data in the quantum state space through a quantum feature map. The choice of which feature map to use is important and may depend on the given dataset we want to classify. A key element of the feature map is not only the use of quantum state space as a feature space but also the way data are mapped into this high dimensional space.

A big challenge in quantum machine learning is how we encode the classical information to quantum states for quantum computing. The kernel method can be implemented to quantum computing by considering the quantum circuit as an encoding function Φ where the quantum feature map is defined as $|\Phi(x)\rangle = U(x)|0\rangle^n$ and the kernel is naturally defined as $K(x_i, x_j) = |\langle\Phi(x_i)|\Phi(x_j)\rangle|^2$. This provides the data points to be mapped into quantum Hilbert space [30], where using quantum computer will have a big advantage. Using quantum circuits, a data $x \in \mathbb{R}^n$ is mapped to an n-qubit quantum feature state $\Phi(x) = U(x)|0\rangle^n \langle 0^n|U^\dagger(x)$ through a unitary circuit $U(x)$, and we can employ the circuit to evaluate the kernel by:

$$K(x_i, x_j) = |\langle\Phi(x_i)|\Phi(x_j)\rangle|^2 = |\langle 0^n|U^\dagger(x_i)U(x_j)|0\rangle^n|^2 \quad (3)$$

The kernel can be estimated on a quantum computer by evolving the initial state $|0\rangle^n$ with $U^\dagger(x_i)U(x_j)$ and counting the frequency of the 0^n outcome. As long as the quantum kernel $K(x_i, x_j)$ can be computed efficiently, we can do optimization in the Hilbert space while other optimization steps can be performed on classical computer. For more details about quantum kernel estimation, please refer to [14].

Constructing feature maps based on quantum circuits that are hard to simulate classically is an important step towards obtaining a quantum advantage over classical approaches. The authors of [14] proposed a family of feature maps that is conjectured to be hard to simulate classically and that can be implemented as short-depth circuits on near-term quantum devices. For some applications, we may want to consider a more general form of the feature map. [14] proposed a number of popular feature maps such as ZFeatureMap and ZZFeatureMap. One way to generate is to use Pauli feature map and specify a set of Pauli gates instead of using the default Z gates. In this paper, we will customize a feature map that has the similar parameters as ZFeatureMap and ZZFeatureMap such as reps and data map function along with an additional Pauli's parameter to change the gate set. The customized feature map will include ZFeatureMap and ZZFeatureMap as special cases. For example, a typical of our customized quantum feature map will be of the form

$$U_{\Phi(\mathbf{x})} = \left(\exp \left(i \sum_{j,k} \phi_{\{j,k\}}(\mathbf{x}) Z_j \otimes Z_k \right) \exp \left(i \sum_j \phi_{\{j\}}(\mathbf{x}) P_j \right) H^{\otimes n} \right)^d$$

where P_j can be one of the rotation gates X, Y, Z . The depth $d = 1$ version of this quantum circuit is shown in Figure 1 below for $n = 2$ qubits.

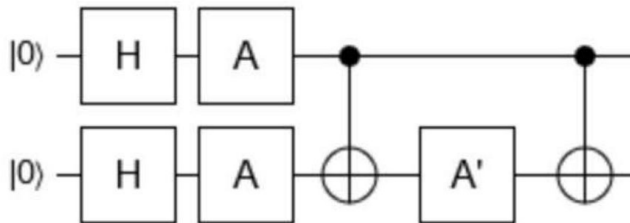


FIG. 1: Quantum circuit for $n = 2$ qubits

The circuit begins with a layer of Hadamard gates $H^{\otimes n}$ followed by a layer of single-qubit $A = e^{i\phi_{\{j\}}(\mathbf{x})P_j}$ gates. The A gates are parametrized by the set of angles $\phi_{\{j\}}(\mathbf{x})$ but around different axes and $\phi_{\{j\}}(\mathbf{x})$ depends on the feature data. The diagonal entangling gate $e^{i\phi_{\{0,1\}}(\mathbf{x})Z_0 \otimes Z_1}$ is parametrized by an angle $\phi_{\{0,1\}}(\mathbf{x})$ and can be implemented using two CNOT gates and one $A' = e^{i\phi_{\{0,1\}}(\mathbf{x})Z_1}$ gate as shown in Figure 1.

It is challenging to design suitable kernel function for different datasets. In this paper we combine genetic algorithm to explore a global optimization method that trains the structure of the quantum circuit. This approach can overcome barren plateaus and other obstacles in traditional optimization and obtain good learning kernels [3, 12].

4. EVOLUTIONARY MULTI-OBJECTIVE OPTIMIZATION

Genetic algorithms represent a powerful class of optimization techniques rooted in the principles of evolution. These algorithms navigate a solution space by evolving a population of individuals, where each individual encodes a feature

map. Through successive iterations or generations, genetic operations guide the selection of offspring to improve one or more objectives. This evolutionary pressure efficiently leads to the selection of well-suited individuals from an extensive configuration space.

The choice of genetic operations is fundamental for the effectiveness and applicability of a genetic algorithm. The selection operator plays a key role by choosing a subset of the existing population to create a new generation through crossover and mutation operations. The mutation operator randomly alters selected individuals' information to explore distant regions of the solution space, while crossover enables more radical explorations by exchanging genetic information between two individuals. Importantly, the probabilities of mutation and crossover are fixed values fine-tuned for optimal performance, whereas the selection probability is proportional to individuals' fitness. To ensure the genetic algorithm's efficiency and convergence, early stopping conditions are employed. These conditions determine whether the evolutionary process has achieved its goals. Potential strategies include checking the convergence or saturation of the fitness objective, maintaining a minimum accuracy threshold to continue the process, or setting a maximum number of generations. By leveraging these essential components, genetic algorithms become a valuable tool for tackling complex optimization tasks in diverse domains.

An Evolutionary Multi-Objective Optimization (EMO) problem involves a number of objective functions which are to be either minimized or maximized. As in a single-objective optimization problem, the multi-objective optimization problem may contain a number of constraints which any feasible solution (including all optimal solutions) must satisfy, see [1, 6, 23] for more details. Since objectives can be either minimized or maximized, we state the multi-objective optimization problem in its general form:

$$\left. \begin{array}{ll} \text{Minimize/Maximize} & f_m(\mathbf{x}), \quad m = 1, 2, \dots, M; \\ \text{subject to} & g_j(\mathbf{x}) \geq 0, \quad j = 1, 2, \dots, J; \\ & h_k(\mathbf{x}) = 0, \quad k = 1, 2, \dots, K; \\ & x_i^{(L)} \leq x_i \leq x_i^{(U)}, \quad i = 1, 2, \dots, n. \end{array} \right\}$$

The optimal solutions in multi-objective optimization can be defined from a mathematical concept of partial ordering. In the parlance of multi-objective optimization, the term domination is used for this purpose. In this paper, we restrict ourselves to discuss unconstrained (without any equality, inequality or bound constraints) optimization problems. The domination between two solutions is defined as follows. A solution $\mathbf{x}^{(1)}$ is said to dominate the other solution $\mathbf{x}^{(2)}$, if both the following conditions are true:

1. The solution $\mathbf{x}^{(1)}$ is no worse than $\mathbf{x}^{(2)}$ in all objectives. Thus, the solutions are compared based on their objective function values (or location of the corresponding points ($\mathbf{z}^{(1)}$ and $\mathbf{z}^{(2)}$) on the objective space).
2. The solution $\mathbf{x}^{(1)}$ is strictly better than $\mathbf{x}^{(2)}$ in at least one objective.

All points which are not dominated by any other member of the set are called the non-dominated points of class one, or simply the non-dominated points. One property of any two such points is that a gain in an objective from one point to the other happens only due to a sacrifice in at least one other objective. This trade-off property between the non-dominated points makes the practitioners interested in finding a wide variety of them before making a final choice. These points make up a front when viewed together on the objective space; hence the non-dominated points are often visualized to represent a non-domination front. If the given set of points for the above task contain all points in the search space (assuming a countable number), the points lying on the non-domination front, by definition, do not get dominated by any other point in the objective space, hence are the Pareto-optimal points (together they constitute the Pareto-optimal front).

Non-dominated Sorting Genetic Algorithm (NSGA-II) was introduced for solving several constrained problems such as a five-objective seven-constraint nonlinear problem. The NSGA-II procedure [6] is one of the popularly used EMO procedures which attempt to find multiple Pareto-optimal solutions in a multi-objective optimization problem.

5. QUANTUM KERNEL FOR SUPPORT VECTOR MACHINE

5.1. Genetic quantum feature map

We will now implement the NSGA-II algorithm that automatically designs and optimizes quantum classifiers based on quantum feature maps and support vector machines. The algorithm explores a configuration space of parameterized quantum circuits that potentially represent feature maps. It looks for those circuits that, once trained in a machine learning method, maximize the accuracy with which they generalize to the validation data set, while minimizing the complexity of the circuit, which is measured in terms of local gates (Hadamard gate and rotation gates) and

CNOT gates. This algorithm decides which individuals survive to the next generation based on Pareto-dominance and density-based metrics. See [3, 8, 11] for additional details.

In the previous studies [3, 11], it is found that the number of entanglement gates are sacrificed by the local gates. To address this problem, we separate CNOT gates from local gates and add two optimizing functions. The first step for engineering our algorithm is to design a map from the genetic information to the quantum circuit that we wish to characterize. In our model, the genes will be binary strings that encode local, entangling and parameterized quantum gates.

We modified the encoding method [3, 11] to create a quantum circuit with a minimum of local and CNOT gates and maximum of accuracy. To simplify the problem, we choose the feature number as the number of qubits (N). Our encoding scheme begins with N number H gates and N possible rotation gates and extra two bits to indicate a rotation with respect to X, Y, Z , followed by possible H entanglement which can be implemented by two rotation gates and a CNOT gates as shown in Figure 1, the last two bits are reserved for repetitions. We also include the data into the encoding. Because the feature number is the same as the number of qubits, thus the i -th gene that operates on the qubits of the quantum register possibly depends on the i -th variable from the input data $\mathbf{x} \in \mathbb{N}^d$. Specifically, rotation gate is parameterized by a value in the input data,

$$R_\alpha(x_k) = \exp(-i\frac{x_k}{2}\sigma^\alpha)$$

where σ^α are one of Paulis = $[X, Y, Z]$. As we see from Figure 1, an entanglement between circuits i, j can be implemented using two CNOT gates and rotation $e^{i\phi_{\{0,1\}}(x)Z_1}$ gate. For the rotation gate of the entanglement implementation between circuits i, j . The rotation parameter is chosen to be $x_i x_j$ as $R_Z(x_i x_j) = \exp(-i\frac{x_i x_j}{2}Z)$.

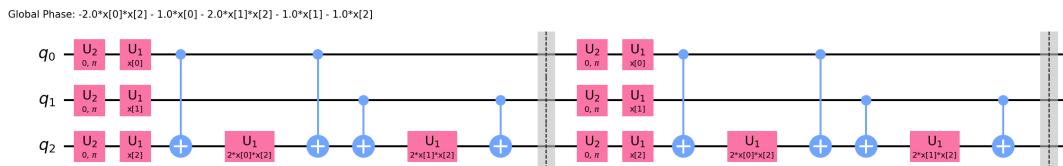


FIG. 2: Example for encoding scheme: the number of qubits is 3, the binary bits are $[1, 1, 1, 1, 0, 0, 1, 1, 1, 0]$, the first three bits for 3 rotation gates, and next two bits indicates the rotation with respect to X, Y, Z , followed 3 bits for possible entanglements, the last two bits is for repetitions.

To demonstrate the encoding scheme that exemplifies all types of gates, we use three qubits and 10 bits per gene as shown in Figure 2. The genetic algorithm process starts with an initial population of individuals, represented by bit strings of size $N + \binom{N}{2} + 4$. The evaluation function decodes each individual, creating an associated quantum circuit. This circuit, together with the training dataset, is used to evaluate the corresponding kernel matrices and then plug them into the SVM algorithms to compute the fitness function. The best individuals have more probability to be elected and subjected to the different genetic operations, such as mutation, crossover and selection, creating a new generation of individuals or quantum circuits. The whole process is repeated until we meet the convergence criteria.

5.2. Fitness functions

Fitness is also considered as objective function or cost function. We pass a solution to this function and it returns the fitness of that solution. In the below multi-objective fitness function (4), we aim to both **maximize the accuracy** and **minimize the gate costs**. A common strategy for multi-objective problem is to find the Pareto front [1, 6, 23] by choosing high domination points with crowd distance techniques. While different gates may have different costs [3, 11, 20], we separate CNOT gates from local gates and add two fitness optimizing functions. The three dimensional Pareto fronts could be used for the strategies of cost-effective trade off. The accuracy is simply the mean accuracy of the given test data and labels, with the SVM model generated by a quantum circuit. Gate costs are calculated by counting the sequence of basic physical operations required for implementation on a quantum computer:

$$\begin{cases} \text{(maximize) Fitness 1} = \text{prediction accuracy} \\ \text{(minimize) Fitness 2} = \text{local gates} = \text{Rgate} + \text{Hgate} \\ \text{(minimize) Fitness 2} = \text{CNOT gate} \end{cases} \quad (4)$$

Our fitness function is designed to maximize the accuracy and minimize the complexity of the variational circuit. To compute this metric, we divide the data into a training set and a test set. We use the quantum circuit and the

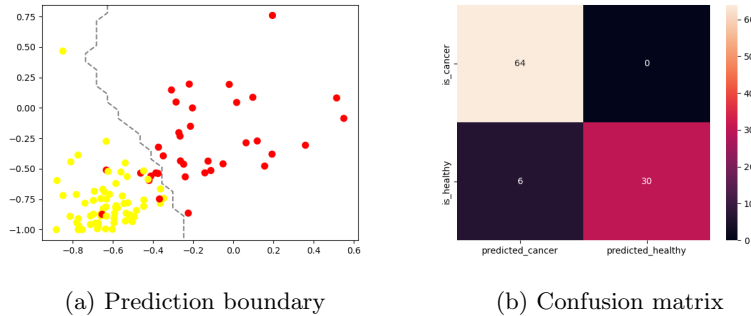


FIG. 3: Prediction boundary and confusion matrix

training set to compute the classifier with the quantum kernel SVM. We then average the accuracy of the model over the test set. The Pareto front created from the genetic process carefully balances the relative importance of both figures of merit. In order to achieve a proper balance, we don't include weights to the objective functions, which could influence the accuracy and numbers of gates.

6. EXPERIMENTS WITH TWO DATASETS

We apply high dimensional NSGA-II along with quantum kernels to two datasets. One is the breast cancer data set which has 30 features and another is the Iris dataset with 4 features. To increase the challenge for high accuracy, we choose not to use a principal component analysis (PCA) for dimension reduction. The training algorithm consists on six steps, which are repeated until convergence. Step 1: first, we create an initial population of individuals as binary chains with $N + \binom{N}{2} + 4$ bits, where N are the maximum number of qubits. Step 2: each individual is decoded and transformed into a quantum circuit. Step 3: using this ansatz circuit, we compute the kernel of a quantum SVM, training a classifier with the training dataset. Step 4: we compute the accuracy of the classifier using the test set. This is the metric which tends to be maximized. Step 5: we compute the effective size of the circuit in terms of the number of local and entangling gates in the circuit. Those are the metric that tends to be minimized. Step 6: based on the three fitness objectives to maximize accuracy and minimize circuit sizes, we apply the genetic algorithm operators of selection, crossover and mutation, producing the next generation of individuals. We then return to step 2 and repeat the process until convergence.

6.1. Breast cancer dataset

First, we consider the breast cancer dataset provided by Sklearn [26, 77]. The breast cancer dataset contains measurements of breast tissue, obtained by a medical imaging technique. From that, several measurements of the cell nuclei are derived. The goal is to determine whether a tumor is benign (harmless) or malignant (that is dangerous, in other words cancer). The breast cancer dataset imported from scikit-learn contains 569 samples with 30 real, positive features (including cancer mass attributes like mean radius, mean texture, mean perimeter, et cetera). Of the samples, 212 are labeled "malignant" and 357 are labeled "benign". We load this data into a 569-by-30 feature matrix and a 569-dimensional target vector, and randomly select a number of features which is the same as the number of quantum circuits and designate 100 rows for training and 50 rows for testing.

With our training and testing datasets ready, we use the procedure above to estimate the training and testing quantum kernel matrices. The quantum kernel can now be plugged into classical kernel methods. Figure 3a depicts data points and prediction boundaries from the quantum kernel SVM for a two qubit case and Figure 3b is for the corresponding confusion matrix which is used to define the performance of a classification algorithm. This provides us with an estimate of the quantum kernel matrix, which we can then use in a kernel for support vector classification.

We compared different kernels and quantum feature map methods together. We computed the four popular classical kernels ('Linear', 'Poly', 'RBF', 'Sigmoid'). For each qubit size, we randomly select 50 combinations of the features with this size, Table 1 and Figure 4 presents the average of the best accuracy for each prediction method with the different number of features/qubits. Comparing the classical kernel methods, quantum kernel generated by genetic algorithm outperforms all classical kernels with the dataset. Also note the RBF kernel outperforms all other classical kernels. It is clear that the quantum kernel is suitable for the dataset.

TABLE 1: Accuracy comparison for kernel methods with breast cancer dataset. The accuracy is calculated as the average of the best accuracies for the 50 randomly selected features.

Kernel Method	Number of features/qubits								
	2	3	4	5	6	7	8	9	10
Linear	0.82	0.86	0.9	0.91	0.93	0.93	0.93	0.94	0.95
Poly	0.83	0.88	0.9	0.91	0.93	0.93	0.93	0.94	0.94
RBF	0.84	0.88	0.9	0.91	0.93	0.93	0.93	0.93	0.94
Sigmoid	0.74	0.75	0.78	0.95	0.82	0.81	0.8	0.82	0.82
Quantum	0.85	0.90	0.93	0.95	0.96	0.96	0.96	0.97	0.97

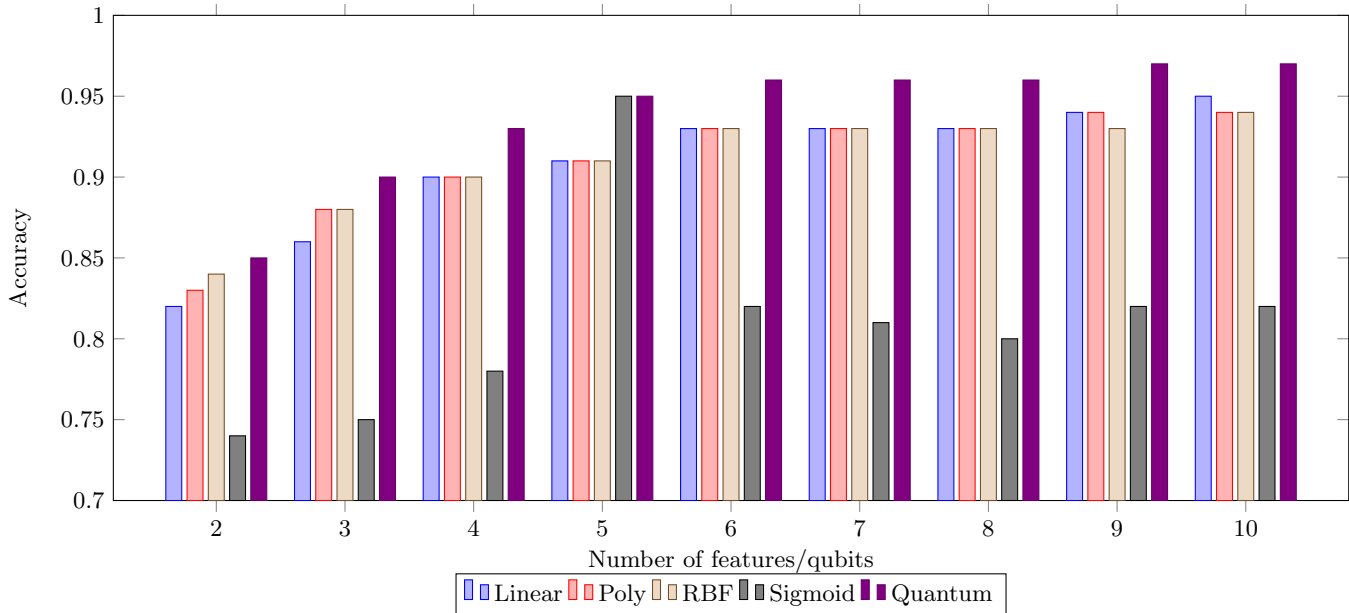


FIG. 4: Accuracy comparison for kernel methods with breast cancer dataset

Figure 6a, 6b, 6c depict the Pareto-optimal fronts in three and two dimensions for one instance. The Pareto fronts explicitly show the strategy to achieve a high accuracy while keeping the gate costs low. The Pareto-optimal fronts allow us to carefully exam cost-effective trade off strategies. In many cases, a large of number of objectives, may be in conflict to each other. The three dimensional Pareto-optimal fronts and their projections in the two dimension spaces give more insights of the significant contributions of entanglements to the accuracy for the quantum kernel.

More importantly, Table 2 and Figure 5 present the corresponding average numbers of local and CNOT gates for the quantum circuits. We observe that CNOT gates are reasonable proportional to the number of local gates in our experiments for the dataset. The result is in contrast to that in [3, 11] where the entanglement gates are largely suppressed. The minimization functions in [3] use weights to balance the relative importance of both figures of merit. As described in [3], high weight in accuracy can produce a collapse into one individual losing the necessary genetic diversity to be able to minimize the quantum circuit size along the evolution. On the other hand, a very small number

TABLE 2: Gate numbers of Quantum feature map with breast cancer data. The gate numbers are calculated as the average gates with the best accuracies of the 50 randomly selected features.

Gate	Number of features/qubits								
	2	3	4	5	6	7	8	9	10
Local gates	11.42	14.98	17.4	24.52	21.46	29.2	31.84	37.18	40.12
CNOT gates	2.48	5.96	10.4	17.36	18.0	26.68	32.16	40.2	45.64

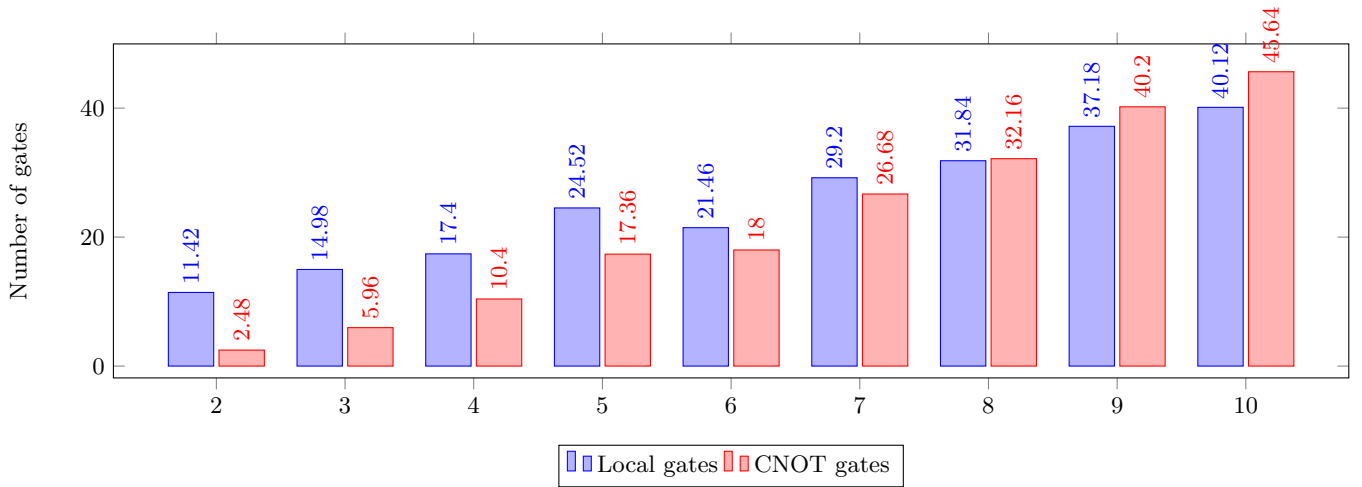


FIG. 5: Gate numbers of Quantum feature map with breast cancer data.

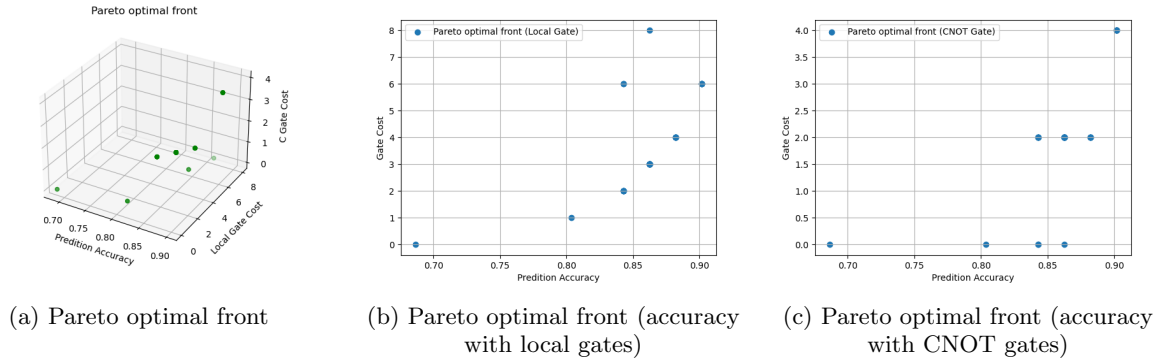


FIG. 6: Three and two dimensional Pareto optimal fronts for breast cancer data

of gates can hinder the power of the quantum kernel to separate the features.

6.2. Iris dataset

TABLE 3: Accuracy comparison for the kernel methods with Iris dataset. The best accuracy for each prediction method with the different features

Kernel Method	Number of features/qubits		
	2	3	4
Linear	0.96	0.99	1
Poly	0.96	0.99	1
RBF	0.95	0.99	1
Sigmoid	0.88	0.94	0.95
Quantum	0.96	0.99	1

Secondly, we consider the Iris dataset consisting of 3 different types of irises' (Setosa, Versicolour, and Virginica) petal and sepal length, stored in a 150x4 arrays. The rows being the samples and the columns being: Sepal Length, Sepal Width, Petal Length and Petal Width. Because there are only 4 features and we choose not to randomly select features. We select 2, 3 and 4 features separately for our test. In fact, there are only 6 features with 2 qubits, and 4 features with 3 qubits and one feature with 4 qubits. We run the same procedure and obtain accuracy and we

TABLE 4: Gate numbers for the quantum kernel method with Iris data. Gate numbers with the best accuracy

Gate	Number of features/qubits		
	2	3	4
Local gates	3.17	4	5
CNOT gates	0	0	0

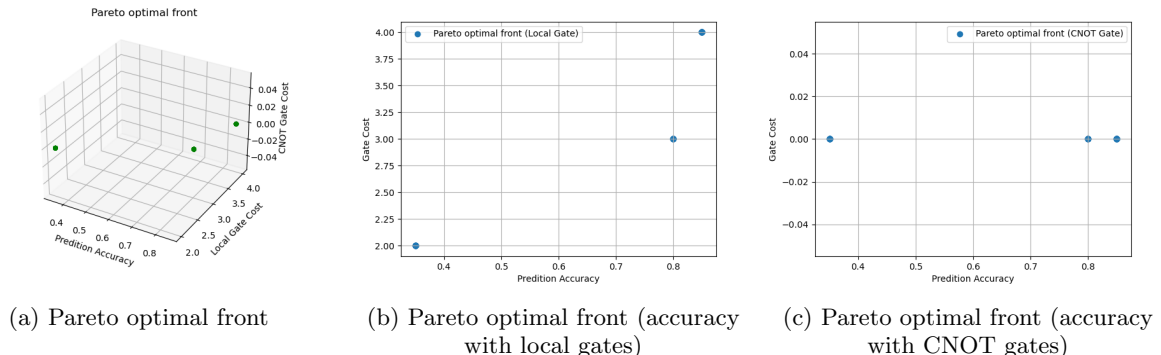


FIG. 7: Three and two dimensional Pareto optimal fronts for Iris data

compare the quantum kernel with the classical SVM kernels.

We use the same procedure as for the breast cancer data, to compare different kernels with the kernel generated from quantum feature map generating. Table 3 presents the best accuracy for each prediction method with the different number of features/qubits. Comparing the classical kernel methods, quantum kernel generated by genetic algorithm performs equally well or outperforms classical kernels with the dataset. Table 4 presents the corresponding numbers of local and CNOT gates for the quantum circuits. For the Iris dataset, it appears that the number of CNOT gates most are zero. It could result from the fact that in this case, the local gates are able to achieve high accuracy and there is no need to include the entanglements. Figure 7a, 7b, 7c depict the Pareto-optimal fronts in three and two dimensions for one instance. The Pareto fronts explicitly show the strategy to achieve a high accuracy while keeping the gate costs low.

6.3. Data separability and non-local gates

In this section we intend to investigate how data complexity, specifically, data separability, affects the number of the entanglement circuits. In machine learning, the performance of a classifier depends on both the classifier model and the separability/complexity of datasets. The distribution of the data and estimates of the shape and size of the decision boundary are among the known measures for this characterization [19]. For comparison, we choose three indexes to quantitatively measure the separability of datasets.

The first index is the separability index (SI) measure which estimates the average number of instances in a dataset that have a nearest neighbor with the same label. Since this is a fraction, the index varies between 0-1 or 0-100%. Another separability measure, based on the class distance or margin is the hypothesis margin index (HMI), introduced in [18]. It measures the distance between an object's nearest neighbor of the same class (near-hit) and a nearest neighbor of the opposing class (near-miss) and sums over these. Margins play a crucial role in modern machine learning research. They measure the classifier confidence when making its decision. Margins are used both for theoretical generalization bounds and as guidelines for algorithm design. This means the larger the near-miss distance and smaller the near-hit values, the larger the hypothesis margin index will be.

$$\theta_P(x) = \frac{1}{2}(\|x - \text{nearmiss}(x)\| - \|x - \text{nearhit}(x)\|)$$

where $\text{nearhit}(x)$ and $\text{nearmiss}(x)$ denote the nearest point to x in P with the same and different label, respectively. Therefore, large hypothesis-margin ensures large sample-margin, and the dataset has high separability.

The third index is the distance-based separability index (DSI) which was recently introduced in [17]. They considered the situation in which different classes of data are mixed in the same distribution to be the most difficult for classifiers to separate. Before introducing the DSI, we introduce the intra-class distance (ICD) and the between-class distance

(BCD) set that are used for computation of the DSI. Suppose X and Y have N_x and N_y data points, respectively. The intra-class distance (ICD) set $\{d_x\}$ is a set of distances between any two points in the same class (X), as: $\{d_x\} = \{\|x_i - x_j\|_2 | x_i, x_j \in X; x_i \neq x_j\}$. The between-class distance (BCD) set $\{d_{x,y}\}$ is the set of distances between any two points from different classes (X and Y), as $\{d_{x,y}\} = \{\|x_i - y_j\|_2 | x_i \in X; y_j \in Y\}$. The metric for all distances is *Euclidean* (l^2 norm). We firstly introduce the computation of the DSI for a dataset containing only two classes X and Y . First, the ICD sets of X and Y : $\{d_x\}, \{d_y\}$ and the BCD set: $\{d_{x,y}\}$ are computed by their definitions. The similarities between the ICD and BCD sets are then computed using the the Kolmogorov–Smirnov (KS) distance

$$s_x = KS(\{d_x\}, \{d_{x,y}\}), \text{ and } s_y = KS(\{d_y\}, \{d_{x,y}\}).$$

Finally, the DSI is the average of the two KS distances:

$$DSI(\{X, Y\}) = \frac{(s_x + s_y)}{2}.$$

TABLE 5: Separability indexes of breast cancer data

Separability Index	Number of features/qubits								
	2	3	4	5	6	7	8	9	10
SI	0.78	0.82	0.84	0.87	0.88	0.88	0.88	0.89	0.90
HMI	4.18	5.82	7.47	8.53	10.82	10.75	11.61	12.46	13.36
DSI	0.27	0.28	0.32	0.34	0.38	0.35	0.35	0.36	0.37

TABLE 6: Separability indexes of Iris data

Separability Index	Number of features/qubits		
	2	3	4
SI	0.9	0.94	0.95
HMI	8.29	10.46	12.19
DSI	0.78	0.80	0.82

For the breast cancer dataset, for each qubit size, we randomly select 50 combinations of the features with this size, Table 5 presents the corresponding average numbers of the three separability indexes along with each number of the features/qubits. For comparison, we calculated the corresponding average three separability indexes for three qubits/features in Table 6 for the Iris dataset (in fact, there are only 6 features with 2 qubits, and 4 features with 3 qubits and one feature with 4 qubits). This comparison of the separability indexes for the two datasets may explain why we need more CNOT gates for the breast cancer dataset. From the definitions, it is clear that *the higher the three indexes are, the easier it is to separate a dataset*. Clearly the separability indexes for the Iris dataset are larger than those of the breast cancer dataset, which explains why the quantum feature maps for the breast cancer dataset needs more CNOT gates to achieve high accuracy. For the Iris data, which has much higher separability indexes, and it seems that the CNOT gates are almost zero. In addition, for the breast cancer dataset, we see that the higher dimensions of features/qubits, the more CNOT gates are needed. This indicates that entanglements may be only needed for lower separability indexes and high dimensional qubits.

7. CONCLUSION AND DISCUSSION

In this paper, we apply multi-objective genetic algorithm, specifically, NSGA-II to construct quantum kernel feature maps for support vector machines. We optimize the quantum feature map of quantum kernels using genetic algorithm. By separating the optimization functions for local gates and non-local gates (CNOT gates), the experiments in this paper demonstrate that the configuration of the quantum kernel maps for support vector machines include a proportional number of CNOT gates for entanglement, which is in contrast to a result in [3, 11] where the CNOT gates are largely suppressed. Entanglement is a concept that's central to quantum mechanics, and understanding its mathematical formulation is key to understanding how it enables quantum computing. Further analysis of the three dimensional set of non-dominated points gives us more insights of the feature map design. Our experiments further indicate that higher dimensional qubits may need more CNOT gates to achieve a high prediction accuracy.

In this paper, three separability indexes are used to identify how data can influence the configuration of the feature maps for the quantum support vector machine. Our experiments indicate that for the same dataset, higher dimensions of qubits may need more CNOT gates to achieve a better prediction accuracy. A dataset with higher separability indexes may need more CNOT gates to achieve high prediction accuracy. The results indicate that various separability indexes can be used to help assess the construct efficient quantum circuits for achieving high accuracy. Currently, the documentation for quantum kernels at qiskit.org do not provide a guide for how these parameters should be chosen. For example, the entanglement parameter of ZZFeatureMap has three options: linear, full and circular. The results of this paper can be used to help choosing these parameters based on analysis of data.

A clear benefit in using quantum kernel estimation to enhance machine learning applications has still to be found [46]. [7, 16] discussed a number of metrics based on the geometric difference of data relates to the feature spaces to identify potential quantum advantage in learning tasks. There is no best model in machine learning which outperforms all others, and efficiency is based on the type of training data distribution. [16] develop a methodology for assessing potential quantum advantage in learning tasks and developed the geometric difference of data as a starting point to evaluate quantum kernel and indicate the presence of a potential quantum advantage. The geometric difference relates to the feature spaces and yields a measure of the separation in prediction errors of the two kernels under scrutiny [7].

Analysis of data separability indicates that the higher the separability of data, the more CNOT gates are needed to achieve high accuracy of prediction. This observation will likely help us design more efficient quantum circuits for machine learning. Future research can further develop more efficient indexes/metrics of data to reveal the presence of a potential quantum advantage. By exploiting the entanglement between qubits, quantum computers can perform optimization and machine learning tasks much faster than classical computers. This has many potential applications, including the optimization of logistics and supply chains, the design of new financial models, and the development of new artificial intelligence algorithms.

The integration of quantum computing with machine learning presents an exciting frontier, with immense potential to transform the landscape of computation and expand the horizons of problem-solving across various domains. As research in this area continues to progress, the transformative impact of quantum machine learning on complex problem-solving remains eagerly anticipated.

-
- [1] E.B. Alaia, I.H. Dridi, H. Bouchriha and P. Borne, *Genetic algorithm with pareto front selection for multi-criteria optimization of multi-depots and multi- vehicle pickup and delivery problems with time windows*, 2014 15th International Conference on Sciences and Techniques of Automatic Control and Computer Engineering, pp. 488-493, (2014).
 - [2] G. Aleksandrowicz et al, *Qiskit: An Open-source Framework for Quantum Computing*, Zenodo, (2019).
 - [3] S. Altares-López, A. Ribeiro, J.J. García-Ripoll, *Automatic design of quantum feature maps*, Quantum Science and Technology, vol. 6, no. 4, (2021).
 - [4] J. Biamonte, P. Wittek, N. Pancotti, P. Rebentrost, N. Wiebe and S. Lloyd, *Quantum machine learning*, Nature 549, pp. 195-202, (2017).
 - [5] A. Baughman, K. Yogaraj, R. Hebbar, S. Ghosh, R.U. Haq and Y. Chhabra, *Study of Feature Importance for Quantum Machine Learning Models*, arXiv:2202.11204, (2022).
 - [6] K. Deb, S. Agrawal, A. Pratap, T. Meyarivan, *A fast and Elitist multi-objective Genetic Algorithm: NSGA-II.*, IEEE Transactions on Evolutionary Computation. 2002;6(2):182-197.
 - [7] Di Marcantonio, Francesco and Incudini, Massimiliano and Tezza, Davide and Grossi, Michele, *Quantum Advantage Seeker with Kernels (QuASK): a software framework to speed up the research in quantum machine learning*, Quantum Machine Intelligence 5 (1), 2023
 - [8] B. Barán, A. Carballude and M. Villagra *Neighbor Optimization of N-Dimensional Quantum Circuits*, SN Computer Science 2, 2021
 - [9] D. Chivilikhin, A. Samarin, V. Ulyantsev, I. Iorsh, A.R. Oganov and O. Kyriienko, *MoG-VQE: Multiobjective genetic variational quantum eigensolver*, arXiv:2007.04424, (2020).
 - [10] P. Chen, L. Yuan, Y. He and S. Luo, *An improved SVM classifier based on double chains quantum genetic algorithm and its application in analogue circuit diagnosis*, Neurocomputing, vol. 211, pp. 202-211, (2016).
 - [11] B.-S. Chen, J.-L. Chern, *Generating quantum feature maps for SVM classifier*, arXiv:2207.11449, (2022).
 - [12] M. Gönen and E. Alpaydin, *Multiple Kernel Learning Algorithms*, Journal of Machine Learning Research, vol. 12, pp. 2211-2268, (2011).
 - [13] J.R. Glick, T.P. Gujarati, A.D. Córcoles, Y. Kim, A. Kandala, J.M. Gambetta and K. Temme, *Covariant quantum kernels for data with group structure*, APS March Meeting 2022, vol. 67, no. 3, (2022).
 - [14] V. Havlíček, A.D. Córcoles, K. Temme, M. Takita, M. Kandala, J.M. Chow and J.M. Gambetta, *Supervised learning with quantum-enhanced feature spaces*, Nature 567, pp. 209-212, (2019).
 - [15] Du Y, Hsieh M H, Liu T and Tao D *Physical Review Research* 2 2020 URL <https://doi.org/10.1103/physrevresearch.2.033125>
 - [16] Huang H-Y, Broughton M, Mohseni M, Babbush R, Boixo S, Neven H, McClean JR *Power of data in quantum machine learning*, Nature Communications (2021) 12(1). <https://doi.org/10.1038/s41467-021-22539-9>

- [17] S. Guan, M. Loew, *A novel intrinsic measure of data separability*, Appl Intell 52, 17734–17750 (2022). <https://doi.org/10.1007/s10489-022-03395-6>
- [18] R. Gilad-Bachrach, A. Navot, N. Tishby, *Margin based feature selection - theory and algorithms*, ICML '04: Proceedings of the twenty-first international conference on Machine learning, July 2004. <https://doi.org/10.1145/1015330.1015352>
- [19] Ana C. Lorena and Luís P. F. Garcia and Jens Lehmann and Marcilio C. P. Souto and Tin Kam Ho *How Complex Is Your Classification Problem?: A Survey on Measuring Classification Complexity* ACM Computing Surveys, 52(5), 2019, <https://doi.org/10.1145/3347711>,
- [20] S. Lee, S.J. Lee, T. Kim, J.S. Lee, J. Biamonte and M. Perkowski, *The cost of quantum gate primitives*, Journal of Multiple-Valued Logic and Soft Computing, vol. 12, No. 5-6. pp. 561-573, (2006).
- [21] Y. Liu, S. Arunachalam and K. Temme, *A rigorous and robust quantum speed-up in supervised machine learning*, Nature Physics, vol. 17, pp. 1013-1017, (2021).
- [22] M. Mafu and M. Senekane, *Design and Implementation of Efficient Quantum Support Vector Machine*, 2021 International Conference on Electrical, Computer and Energy Technologies, pp. 1-4, (2021).
- [23] K. Miettinen, *Nonlinear Multiobjective Optimization*, Boston: Kluwer; 1999.
- [24] S. Moradi, C. Brandner, C. Spielvogel, D. Krajnc, S. Hillmich, R. Wille, W. Drexler and L. Papp, *Clinical data classification with noisy intermediate scale quantum computers*, Scientific Reports, vol. 12, no. 1851, (2022).
- [25] J.E. Park, B. Quanz, S. Wood, H. Higgins and R. Harishankar, *Practical application improvement to Quantum SVM: theory to practice*, arXiv:2012.07725, (2020).
- [26] F. Pedregosa, G. Varoquaux and A. Gramfort et al, *Scikit-learn: Machine Learning in Python*, Journal of Machine Learning Research, vol. 12, pp. 2825-2830, (2011).
- [27] P. Rebentrost, M. Mohseni, and S. Lloyd, *Quantum Support Vector Machine for Big Data Classification*, Physical Review Letters 113, 130503, (2014).
- [28] M. Schuld, N. Killoran *Is quantum advantage the right goal for quantum machine learning?* PRX Quantum 3:030101. (2022) <https://doi.org/10.1103/PRXQuantum.3.030101>
- [29] M. Schuld, *Quantum machine learning models are kernel methods*, arXiv:2101.11020, (2021).
- [30] M. Schuld and N. Killoran, *Quantum Machine Learning in Feature Hilbert Spaces*, Physical Review Letters 122, 040504, (2019).
- [31] M. Schuld, I. Sinayskiy and F. Petruccione, *An introduction to quantum machine learning*, Contemporary Physics, vol. 56, (2015).
- [32] Y. Suzuki, H. Yano, Q. Gao, S. Uno, T. Tanaka, M. Akiyama and N. Yamamoto, *Analysis and synthesis of feature map for kernel-based quantum classifier*, Quantum Machine Intelligence, vol. 2, no. 9, (2020).
- [33] J. R. McClean, S. Boixo, V. N. Smelyanskiy, R. Babbush, and H. Neven *Barren plateaus in quantum neural network training landscapes* Nature Communications, 9 (2018), URL <https://doi.org/10.1038/s41467-018-07090-4>
- [34] R. Li, U. Alvarez-Rodriguez, L. Lamata, and E. Solano *Quantum Measurements and Quantum Metrology* 2017 4 1–7 ISSN 2299-114X
- [35] L. Lamata, U. Alvarez-Rodriguez, J. D. Martín-Guerrero, M. Sanz, and E. Solano 2018 *Quantum Science and Technology* 4 014007 ISSN 2058-9565 URL <http://dx.doi.org/10.1088/2058-9565/aae22b>
- [36] D. Chivilikhin, A. Samarin, V. Ulyantsev, I. Iorsh, A. R. Oganov, and O. Kyriienko 2020 *Mog-vqe: Multiobjective genetic variational quantum eigensolver (Preprint 2007.04424)*
- [37] G. Mengoni and A. Di Pierro, *Quantum feature maps with entangled states*, arXiv:1912.03674, (2019).
- [38] M. Schuld and I. Petruccione, *Quantum natural gradient*, Physical Review A, 103(3), 032630 (2021).
- [39] K. Mitarai, M. Negoro, M. Kitagawa, and K. Fujii, *Quantum circuit learning*, Physical Review A, 98(3), 032309 (2018).
- [40] A. Abbas, D. Sutter, C. Zoufal, A. Lucchi, A. Figalli, and S. Woerner, *The power of quantum neural networks*, Nature Computational Science, 1(6), 403-409 (2021).
- [41] J.R. McClean, S. Boixo, V.N. Smelyanskiy, R.B.abbasne, A.W. Harrow, I.L. Markov, and T. Monz, *Barren plateaus in quantum neural network training landscapes*, Nature Communications, 9(1), 4812 (2018).
- [42] Z. Holmes, R. Schmied, and P. F. O'Malley, *Breakdown of training in deep quantum learning*, Quantum, 5, 462 (2021).
- [43] Z. Wang, A. Chia, Z. Wang, Y. Gong, J. Roland, and S. Lloyd, *Training quantum circuits with projective measurement*, arXiv:2106.11495, (2021).
- [44] A. Arrasmith, M. Cerezo, P. Czarnik, L. Cincio, and P.J. Coles, *Effect of barren plateaus on gradient-free optimization*, Quantum, 5, 558 (2021).
- [45] Z. Holmes, K. Sharma, and P.F. O'Malley, *Expressibility and entangling capability of parameterized quantum circuits for hybrid quantum-classical algorithms*, Physical Review Research, 4(3), 033099 (2022).
- [46] M. Schuld and N. Killoran, *Quantum machine learning for the quantum class*, arXiv:2201.01548, (2022).
- [47] L. Liu and P. Rebentrost, *An adaptive quantum algorithm for linear systems of equations*, arXiv:1811.05371, (2018).
- [48] K. Bartkiewicz, G. Chimini, M. Cianciaruso, A. C. Bertrand, and D. Wisniewski, *Experimental realization of quantum kernels*, Physical Review Letters, 125(10), 100503 (2020).
- [49] A. Paszke, S. Gross, F. Massa, A. Lerer, J. Bradbury, G. Chanan, T. Killeen, Z. Lin, N. Gimelshein, L. Antiga, et al, *PyTorch: An imperative style, high-performance deep learning library*, Advances in Neural Information Processing Systems, 8024-8035 (2019).
- [50] F. Chollet et al, *Keras, GitHub*, <https://github.com/fchollet/keras>.
- [51] V. Bergholm, J. Izaac, M. Schuld, C. Gogolin, M. Broughton, and N. Killoran, *PennyLane: Automatic differentiation of hybrid quantum-classical computations*, arXiv:1811.04968, (2018).
- [52] A. Anis, T. Bromley, J. Broughton, J. Izaac, T. Killoran, C. Bergholm, N. Cottrell, S. Gidney, T. Gokyigit, S. Guha, et al, *Tensorflow quantum: A software framework for quantum machine learning*, arXiv:2101.01178, (2021).

- [53] M. Broughton, M. Schuld, T. Farrow, M. Benenti, and D. Egger, *High performance quantum circuit simulator for OpenQASM 3.0*, *arXiv:2012.09895*, (2020).
- [54] N. Killoran, J. Izaac, M. Quesada, and S. McArdle, *Strawberry fields: A software platform for photonic quantum computing*, *Quantum*, 3, 129 (2019).
- [55] Baidu Quantum Team, *Paddle quantum: A quantum machine learning framework*, *GitHub*, <https://github.com/PaddlePaddle/Quantum>.
- [56] M. Lipow, *A program development and maintenance costs taxonomy*, *Communications of the ACM*, 25(7), 462-464 (1982).
- [57] A. Trisovic, J. Tschoop, P. Robinson, A. Romoser, S. Scott, J. Mangelson, J. Martel, D. Rigby, E. Toczyski, D. Jensen, et al, *Reproducibility in machine learning for health care*, *arXiv:2212.00812*, (2022).
- [58] P. Mineault and T. Nozawa, *Designing reproducible computational workflows*, *arXiv:2110.08655*, (2021).
- [59] T. Botvinik-Nezer, F. Holzmeister, C.F. Camerer, A. Dreber, J. Huber, M. Johannesson, M. Kirchler, J. I. Krajbich, G. Poldrack, T. Schonberg, et al, *Variability in the analysis of a single neuroimaging dataset by many teams*, *Nature*, 582(7810), 84-88 (2020).
- [60] M. A. Campos and M. G. Souto, *The challenges of code maintenance and reuse in scientific research software*, *Journal of Systems and Software*, 172, 110793 (2021).
- [61] B. Schölkopf, R. Herbrich, and A.J. Smola, *A generalized representer theorem*, In *Conference on Learning Theory*, 416-426 (2001).
- [62] F. Pérez-Cruz and O. Bousquet, *Generalized kernel matrices*, *Advances in Neural Information Processing Systems*, 1041-1048 (2004).
- [63] J.L. Rojo-Álvarez, A. Muñoz, M. Maudes, and C. Jutten, *Functional component analysis for functional data*, *Chemometrics and Intelligent Laboratory Systems*, 176, 91-98 (2018).
- [64] G. Camps-Valls, *Kernel methods in hyperspectral image analysis*, *IEEE Signal Processing Magazine*, 23(2), 135-141 (2006).
- [65] A. Ben-Hur, D. Horn, H. Siegelmann, and V. Vapnik, *Support vector clustering*, *Journal of Machine Learning Research*, 2, 125-137 (2008).
- [66] Y. Wang and J. Qi, *Nonlinear manifold learning for image restoration*, *IEEE Transactions on Image Processing*, 23(7), 2946-2957 (2014).
- [67] J. Yang, *Kernel eigenfaces vs. kernel fisherfaces: Face recognition using kernel methods*, *Proceedings of the 2001 IEEE Computer Society Conference on Computer Vision and Pattern Recognition*, 2, II-II (2001).
- [68] H. Huang, K. Sharma, M. Sotiropoulos, and P.F. O'Malley, *Prediction of the output of quantum systems with variational quantum kernels*, *arXiv:2105.09449*, (2021).
- [69] H. Huang, K. Sharma, M. Sotiropoulos, and P.F. O'Malley, *Predicting the properties of molecular systems using quantum kernels*, *Quantum*, 6, 445 (2022).
- [70] L. Liu, J. Bian, P. Rebentrost, and K. Wang, *Learning from distributions based on the discrete logarithm*, *Physical Review Research*, 3(4), 043288 (2021).
- [71] A. Di Pierro and P. Rebentrost, *A quantum support vector machine for small feature spaces*, *arXiv:1810.05867*, (2018).
- [72] A. Di Pierro and M. Incudini, *Quantum machine learning and fraud detection. Protocols, Strands, and Logic*, Springer, Cham, Germany, 139-155 (2021).
- [73] M. Grossi, N. Ibrahim, V. Radescu, R. Loredó, K. Voigt, C. Von Altrock, and A. Rudnik, *Mixed quantum-classical method for fraud detection with quantum feature selection*, *arXiv:2208.07963*, (2022).
- [74] O. Kyriienko and H. Magnusson, *Hybrid quantum-classical classifier with dimensionality reduction for anomaly detection*, *arXiv:2206.16613*, (2022).
- [75] S. Krunić, M. Gastegger, K. Sharma, P. O'Malley, S. Imajo, A. Aspuru-Guzik, and T. E. O'Brien, *Improving the effectiveness of pharmaceutical treatments with quantum kernels*, *arXiv:2202.02108*, (2022).
- [76] E. Peters, C. Pehlevan, C. Campagne-Ibarcq, B. Hacker, A. Chia, J. Bollinger, and S. Lloyd, *A kernel approach to the classification of quantum noise*, *npj Quantum Information*, 7(1), 1-6 (2021).
- [77] Zwitter, Matjaz and Soklic, Milan. *Breast Cancer*. *UCI Machine Learning Repository* (1988). <https://doi.org/10.24432/C51P4M>.